

# Interference-Aware Radio Resource Allocation in D2D Underlying LTE-Advanced Networks

Shaoyi Xu<sup>1,2</sup>, Kyung Sup Kwak<sup>3</sup> and Ramesh R. Rao<sup>4</sup>

<sup>1</sup> School of Electronic and Information Engineering, Beijing Jiaotong University, Beijing, 100044, P. R. China

<sup>2</sup> State Key Laboratory of Integrated Services Networks, Xidian University, Xian, 710071, P. R. China

[e-mail: shyxu@bjtu.edu.cn]

<sup>3</sup> UWB Research Center, Inha University, Incheon, 402-751, Korea

[e-mail: kskwak@inha.ac.kr]

<sup>4</sup> Department of Electrical and Computer Engineering, University of California,

San Diego, La Jolla, CA 92093 USA

[e-mail: rrao@cw.cucsd.edu]

\*Corresponding author: Shaoyi Xu

*Received February 24, 2014; revised May 16, 2014; accepted June 18, 2014; published August 29, 2014*

---

## Abstract

This study presents a power and Physical Resource Blocks (PRBs) joint allocation algorithm to coordinate uplink (UL) interference in the device-to-device (D2D) underlying Long Term Evolution-Advanced (LTE-A) networks. The objective is to find a mechanism to mitigate the UL interference between the two subsystems and maximize the weighted sum throughput as well. This optimization problem is formulated as a mixed integer nonlinear programming (MINLP) which is further decomposed into PRBs assignment and transmission power allocation. Specifically, the scenario of applying imperfect channel state information (CSI) is also taken into account in our study. Analysis reveals that the proposed PRBs allocation strategy is energy efficient and it suppresses the interference not only suffered by the LTE-A system but also to the D2D users. In another side, a low-complexity technique is proposed to obtain the optimal power allocation which resides in one of at most three feasible power vectors. Simulations show that the optimal power allocation combined with the proposed PRBs assignment achieves a higher weighted sum throughput as compared to traditional algorithms even when imperfect CSI is utilized.

---

**Keywords:** device-to-device (D2D) communication, radio resource allocation, Long Term Evolution-Advanced (LTE-A), Physical Resource Block (PRB), mixed integer nonlinear programming (MINLP), weighted sum throughput

---

This work was supported by Important National Science & Technology Specific Projects of China under Grant 2012ZX03003013-003, National Natural Science Foundation of China under Grant 61101138, Beijing Natural Science Foundation with Grant 4132041 and the Fundamental Research Funds for the Central Universities with Grant 2012JBM007. This work was also supported by MSIP, Korea, under the ITRC support program (NIPA-2014-H0301-14-1042) supervised by the NIPA.

<http://dx.doi.org/10.3837/tiis.2014.08.003>

## 1. Introduction

There are some new trends in current mobile smart terminals, context-aware applications for example, are regarded as one of the most important value added services. Besides, social networks and machine-to-machine (M2M) applications are growing fast and changing people's life greatly. In another side, the explosive growth of the mobile user population and multimedia services are faster than the spectrums that service providers can obtain and thus cause a severe overload problem in the current cellular networks. Driven by the new services and to cater for the higher data rate and system capacity required by Long Term Evolution-Advanced (LTE-A), the Third-Generation Partnership Project (3GPP) defined device-to-device (D2D) communications underlying LTE networks as a critical solution which has received much attention recently [1]-[4].

Unlike the infrastructure based cellular network, D2D users (user equipments or mobile terminals) do not communicate via the central coordinator (base station, NodeB or evolved NodeB) but operate as an underlay and communicate directly with each other or more hops. Enabling D2D communication in local cellular networks can obtain many advantages: system spectral efficiency enhancement, user equipments' (UEs) power saving, plug-and-play convenience and new services availability [1]-[4].

However, integrating this new feature in the LTE-A network imposes some new challenges among which interference coordination is one of the most critical issues. Reusing radio resources with LTE-A networks, intra-cell interference is no longer negligible and such interference exists for sharing uplink (UL) and downlink (DL) frequency resources with cellular systems. Due to heavier traffic and fast resource scheduling in DL transmission, sharing UL frequency resources with cellular networks is a preferred solution for D2D communications [2], [5]-[7]. However, interference management is a critical issue in such a hybrid system. As Fig. 1 illustrates, in UL transmission the victim cellular device is the base station (evolved Node B, i.e. eNB in the LTE system) and D2D communication will be exposed to the interference from proximate cellular UEs (CUEs) as well. Such interference must be coordinated to maintain the target system performance.

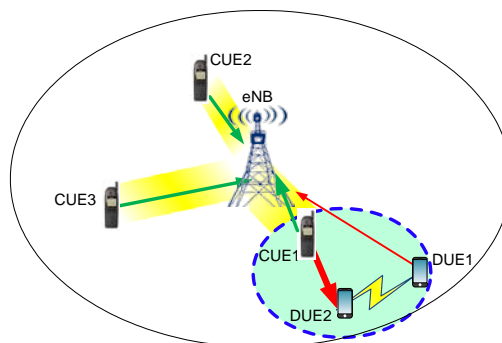


Fig. 1. Illustration of interference when reusing UL spectrums.

To realize the promises of D2D communications and to tackle the intra-cell interference, a number of interference mitigation techniques are proposed in the literature. Aiming to

guarantee the performance of licensed cellular users or maximize the sum throughput of the D2D subsystem, power control and resource allocation schemes are developed in [5]-[8]. Under different constraints and resource sharing methods, the original optimization question is formulated and further solved using Lagrangian Duality Optimization (LDO) with Karush–Kuhn–Tucker (KKT) conditions [5]-[7] or Game theory [5], [8]. To manage the interference between D2D and cellular networks, in [9], a transmit beamforming approach is designed at the D2D transmitter to maximize the throughput of D2D communication based on the estimated channel state information (CSI). Multiple-Input and Multiple-Output (MIMO) based methods are suggested in [10] to deal with the intra-cell interference by designing appropriate precoding or utilizing a column generation method [11]. Authors in [12] applied a mode selection and resource allocation scheme based on particle swarm optimization to maximize the system throughput. A joint transmission mode selection and scheduling scheme is also developed to mitigate the interference [13], [14]. In [15], the authors put up with a partial time-frequency resource allocation framework for D2D communications by that D2D users share partial resources with CUEs instead of whole resources to avoid the intra-cell and inter-cell interference.

However, most of the aforementioned researches deal with the interference mitigation by considering the cellular devices to be the victims and the objective function is devised to maximize the profit of the cellular network nevertheless belittling the D2D users. Consequently, the interference coordination strategy improves the performance of the cellular system at the cost of the reliability of the D2D communication. Therefore, the motivation of our work is to develop an effective scheme sharing cellular UL radio resources by allocating frequencies and transmission power meanwhile maintaining the target weighted sum throughput of the hybrid network. Furthermore, the scenario of applying imperfect CSI is specifically taken into account to reduce the signaling overhead.

Different from the previous researches, our main contributions are summarized as follows.

1) Instead of using the direct sum throughput of the D2D subsystem and the LTE-A network, we use the weighted sum throughput which is considered to be a better metric combining the fairness and energy saving between these two subsystems.

2) We design an effective frequency resources allocation strategy by which the interference not only suffered by the LTE-A system but also to the D2D subsystem can be mitigated effectively. Simulation results prove that lower transmission power can be adopted by using the proposed frequency resources allocation mechanism.

3) Moreover, we develop an efficient power allocation algorithm for sharing UL resources. This problem is formulated as a mixed integer nonlinear programming (MINLP) where frequency resources and transmission power are optimized jointly. Instead of using the traditional optimization solution like the Lagrange Dual Method which has high computational complexity to solve our problem, this optimization problem is resolved efficiently by using three lemmas and one theorem. Furthermore, we finally delimit the optimal power allocation resides in one of at most three power vectors which is helpful for the operators to decrease the system complexity greatly.

4) Specifically, considering the high signaling overhead to obtain perfect channel state information, the case of imperfect CSI is taken into account to extend our proposed scheme into a real scenario. Simulations verify the efficacy of the proposed scheme even in the imperfect CSI scenario.

This work is organized as follows. Section 2 describes the system model and formulates the addressed problem. Section 3 first presents the proposed radio resource allocation scheme and

then the optimization problem is reformulated and resolved in Section 4. Simulation results are shown in Section 5 and the main conclusions are summarized in Section 6.

## 2. System Model and Problem Formulation

We consider the single cellular LTE-A network based on orthogonal frequency division multiple access (OFDMA) where cellular devices and D2D users share UL spectrums. We also assume that the eNB controls the resource allocation in the hybrid system so that non-overlapping resources are allocated within the LTE-A subsystem. Although distributed resource management is also designed in a D2D underlaying cellular systems [5], [16], there are manifold benefits of enabling D2D communication in a LTE-A network under the control of an eNB. Under the control of an eNB, the interference can be restricted effectively and efficiently so that the operators may offer more new services with new revenue opportunities [17]. In another side, for the D2D subsystem, notwithstanding overlapping resources may be used for different D2D pairs, accumulative interference to the cellular victims will be serious. Hence, in our work, non-overlapping resources are also allocated in the D2D subsystem which can be ensured by a Carrier Sense Multiple Access with Collision Avoidance (CSMA/CA) type random access mechanism [2]. We define the used frequency resource as a physical resource block (PRB) which occupies 1 transmission time interval (TTI), i.e. 0.5 milliseconds in the time domain and 180kHz in the frequency domain with subcarrier spacing of 15kHz [18]. In addition, both CUEs and D2D UEs (DUEs) are synchronized with the eNB which means their transmission is aligned to the eNB. An information theoretic approach is adopted for the design of resource allocation therefore the buffers at the eNB are assumed to be always full and all transceivers are equipped with a single antenna.

We assume that the total frequency bandwidth is divided into  $N$  PRBs each of them with the bandwidth  $B$ . Let  $\sigma_n^2$  be the received power of the additive white Gaussian noise (AWGN) on PRB  $n$  and we assume that all users observe the same noise power. The received signal-to-interference-and-noise ratio (SINR) on PRB  $n$  for D2D pair  $m$  can be expressed as

$$\gamma_{m,n}^{DUE} = \frac{P_{m,n} h_{m,n} g_{m,n}^{DUE}}{P_{l,n} h_{l,m,n} g_{l,m,n}^{DUE} + \sigma_n^2} \quad (1)$$

where  $h_{m,n}$  and  $h_{l,m,n}$  represent respectively the small-scale channel gain of D2D pair  $m$  on PRB  $n$  and that from the  $l$ th CUE to the  $m$ th DUE on PRB  $n$ .  $P_{m,n}$  and  $P_{l,n}$  mean the transmission power of the D2D transmitter  $m$  and the  $l$ th CUE on PRB  $n$ .  $g_{m,n}^{DUE}$  and  $g_{l,m,n}^{DUE}$  are path loss functions between the  $m$ th D2D pair and from the  $l$ th CUE to the  $m$ th D2D receiver. Similarly, the SINR of the eNB is

$$\gamma_{l,n}^{eNB} = \frac{P_{l,n} f_{l,n} g_{l,n}^{eNB}}{P_{m,n} f_{m,l,n} g_{m,l,n}^{eNB} + \sigma_n^2} \quad (2)$$

where  $f_{l,n}$  and  $f_{m,l,n}$  respectively denote the small-scale channel gain between the  $l$ th CUE and the eNB and that from the  $m$ th DUE to the eNB on PRB  $n$ .  $g_{l,n}^{eNB}$  and  $g_{m,l,n}^{eNB}$  separately denote the path loss functions for the path between the  $l$ th CUE and the eNB and from D2D pair  $m$  to

the eNB. In our work, we assume  $f$  and  $h$  follow Rayleigh fading and denote  $g = \|v\|^{-\theta}$  with respect to the distance of  $v$  and  $\theta$  is the path loss exponent.

There are some works which deal with system sum throughput in a single cell or multi-cell networks [8], instead of applying the direct sum throughput of the D2D subsystem and LTE networks, the weighted sum throughput is defined in our work. Denote  $\omega_n$  and  $(1-\omega_n)$  the priority weights of a D2D user and a cellular device which use PRB  $n$ . It also can be a user-dependent priority indicator required to be the fairness indicator by the D2D or the LTE-A subsystem. To use the weights is based on the consideration that the operators support both D2D users and cellular users by adopting valid charging methods but offering different services according to different priorities. Furthermore, fairness and energy saving can be obtained in the hybrid system by adjusting  $\omega_n$  appropriately. Accordingly, the proposed weighted sum throughput is expressed as follows

$$\begin{aligned}
R &= \sum_{n=1}^N R_n = \sum_{n=1}^N \left( \omega_n R_n^{DUE} + (1-\omega_n) R_n^{LTE} \right) \\
&= B \sum_{n=1}^N \left( \sum_{m=1}^M \omega_n \log_2(1 + \gamma_{m,n}^{DUE} x_{m,n}) + \sum_{l=1}^L (1-\omega_n) \log_2(1 + \gamma_{l,n}^{eNB} x_{l,n}) \right) \\
&= B \sum_{n=1}^N \sum_{m=1}^M \omega_n \log_2 \left( 1 + \frac{P_{m,n} h_{m,n} g_{m,n}^{DUE}}{P_{l,n} h_{l,m,n} g_{l,m,n}^{DUE} + \sigma_n^2} \right) x_{m,n} \\
&\quad + B \sum_{n=1}^N \sum_{l=1}^L (1-\omega_n) \log_2 \left( 1 + \frac{P_{l,n} f_{l,n} g_{l,n}^{eNB}}{P_{m,n} f_{m,l,n} g_{m,l,n}^{eNB} + \sigma_n^2} \right) x_{l,n}
\end{aligned} \tag{3}$$

where  $x_{i,n}$  is a binary variable,  $x_{i,n} = 1$  represents the UE  $i$  utilizes PRB  $n$  and  $x_{i,n} = 0$  otherwise.  $M$  and  $L$  respectively denote the total number of active DUEs and CUEs. In our work, we aim to maximize the weighted sum throughput by jointly allocating PRBs and transmission power of the DUE and the cellular device which share PRB  $n$ .

To guarantee the quality of service (QoS) of the hybrid system, PRB  $n$  is allowed to be utilized when the SINR is beyond the target value  $\gamma_n^{tgt}$ . Thus, we formulate the objective function for jointly optimizing transmission power and PRBs allocation as

$$\text{maximize } R \tag{4}$$

$$\text{s.t. } \gamma_m^{DUE} \geq \gamma_{DUE}^{tgt}, \forall m \tag{C1}$$

$$\gamma_l^{eNB} \geq \gamma_{eNB}^{tgt}, \forall l \tag{C2}$$

$$P_{m,n} \leq P_{\max}^{DUE}, \forall m, n \tag{C3}$$

$$P_{\min}^{CUE} \leq P_{l,n} \leq P_{\max}^{CUE}, \forall l, n \tag{C4}$$

$$\sum_{m=1}^M x_{m,n} \leq 1, \forall n \tag{C5}$$

$$\sum_{l=1}^L x_{l,n} \leq 1, \forall n \tag{C6}$$

$$x_{i,n} \in \{0, 1\}. \tag{C7}$$

The objective function maximizes the weighted sum throughput. Constraints (C1) and (C2) require the SINR of cellular and D2D users to exceed the target QoS values. (C3) and (C4)

force the transmission power of each user to be below the pre-defined power limit, specifically, for each CUE minimum power is expected for the required QoS. (C5) and (C6) state the CUEs and DUEs respectively operate in the non-overlapping PRBs to perform their transmission.

### 3. Proposed PRBs Allocation Scheme

The aforementioned MINLP is an NP-hard problem and notoriously hard to solve otherwise impossible during a short scheduling period (at least 3 milliseconds in an LTE-A system) [18]. Therefore, a suboptimal heuristic algorithm is proposed in this section by which appropriate PRBs are selected firstly and then the optimal transmission power is determined to satisfy the objective function. In the following, we will first describe the PRBs allocation scheme and then consider the optimal transmission power to maximize the weighted sum throughput for sharing UL resources. Finally we develop a protocol combining the PRBs allocation and power determination in a practical LTE-A system.

The key point of our PRBs allocation is to find the interference region (IR) of each active DUE and orthogonal resources are used in the IR but reused frequencies are allocated outside the IR. Here an IR is defined as the region where a DUE will suffer interference from the nearby CUEs. Furthermore, in our work all PRBs are classified into Bad PRBs (BPRBs) and Suitable PRBs (SPRBs) by the eNB by measuring the UL Reference Signals (RSs). We define the SPRB as the PRB which has a high channel gain between the UE and the eNB. On the contrary, a BPRB has a low channel gain from the UE to the eNB. In the IR, the eNB allocates SPRBs for the LTE-A subsystem but BPRBs to D2D transmission. Outside the IR, PRBs are shared by the DUEs and CUEs. We should note that BPRBs and SPRBs are detected based on the channel quality from the UE to the eNB instead of other links. As a result, even a BPRB is used by D2D transmission, it will not lead to worse performance considering the fact that the distance between two DUEs is short and the channel quality between them is usually good. Consequently, the interference suffered by the LTE-A system and to the D2D users is mitigated simultaneously.

Considering the D2D subsystem is an ad-hoc like system, in our work we assume a CSMA/CA type MAC protocol to be applied for D2D transmission and a dedicated common control channel (CCCH) is used for the D2D handshaking procedure [2]. As a dedicated control channel, there is always signaling transmitted on CCCH during the complete data transmission. Hence, by detecting signals on CCCH, a CUE can find neighboring DUEs and determine the IR for each D2D pair.

#### 3.1 Determination of Interference Region

Naturally, because of the UE's mobility, we model such randomness as a Poisson Point Process (PPP) with the intensity of  $\lambda_M$ . Furthermore, the probability density function (pdf) of a UE with respect to the distance  $v$  between the D2D pair and the CUE is given by  $f(v) = 2\pi\lambda_M v \exp(-\lambda_M \pi v^2)$ . Thus, for a predefined SINR threshold  $T$  received by a CUE, the IR probability can be expressed by averaging the probability when the received power by a CUE on CCCH is higher than  $T$  as

$$p(T, \lambda_M, \theta) = E_v \left[ P[SINR > T | v] \right] = \int_{v>0} P[SINR > T | v] f_v(v) dv. \quad (5)$$

As assumed above,  $f$  and  $h$  follow Rayleigh fading such that the received power by a CUE

follows the exponential distribution with mean  $1/\mu$ . One very useful consequence of the Rayleigh fading model and the definition of the SINR is that, for a fixed distance from the transmitter, the probability of being higher than a threshold can be expressed as a product of Laplace transforms of independent random variables [19]. Specifically, when the transmission power of all transmitters is same we may further obtain that [19]

$$\begin{aligned} p(T, \lambda_M, \theta) &= 2\pi\lambda_M \int_{v>0} \exp(-\pi\lambda_M v^2) \exp(-\mu T \sigma^2 v^\theta) L_I(\mu T v^\theta) v dv \\ &= 2\pi\lambda_M \int_0^\infty \exp\left(\left(-\pi\lambda_M v(1 + \rho(T, \theta)) - \mu T \sigma^2 v^{\theta/2}\right) dv\right) \end{aligned} \quad (6)$$

where  $\rho(T, \theta) = T^{2/\theta} \int_{T^{2/\theta}}^\infty \frac{1}{1+u} \frac{1}{\theta/2} du$  and  $L_I(v)$  is the Laplace transforms of the interference.

### 3.2 Effective PRBs Allocation Scheme

To ensure the valid PRBs allocation, the eNB uses the following policies:

- 1) In the IR, the eNB allocates the SPRBs to CUEs whilst identifies the BPRBs and allocates them to the DUE. Let  $\mathbf{F}_m = (f_{\alpha_{1,m}}^m, f_{\alpha_{2,m}}^m, \dots, f_{\alpha_{N,m}}^m)$  denote the channel gain for the  $m$ th DUE where  $\alpha_1, \alpha_2, \dots, \alpha_N$  are the sequence numbers of BPRBs and we have  $f_{\alpha_{1,m}}^m \leq f_{\alpha_{2,m}}^m \leq \dots \leq f_{\alpha_{N,m}}^m$ . Similarly, the channel gain for the  $l$ th CUE is represented as  $\mathbf{H}_l = (h_{\beta_{1,l}}^l, h_{\beta_{2,l}}^l, \dots, h_{\beta_{N,l}}^l)$  and  $\beta_1, \beta_2, \dots, \beta_N$  are the sequence numbers of SPRBs with  $h_{\beta_{1,l}}^l \geq h_{\beta_{2,l}}^l \geq \dots \geq h_{\beta_{N,l}}^l$ . Thus, the eNB allocates PRB  $n$  to CUE  $l$  when  $n = \max_{n \in H_l} h_{\beta_n}^l$  and PRB  $k$  to DUE  $m$  when  $k = \min_{k \in F_m} f_{\alpha_k}^m$  with  $n \neq k$ .
- 2) Within the IR, if a BPRB of the DUE is same to the SPRB of a CUE, the eNB assigns this PRB to the CUE as a SPRB to guarantee the QoS of the cellular users and allocates the next smallest BPRB to the DUE.
- 3) Outside the IR, the eNB allocates the BPRBs to the CUEs which have large distance to the DUE thus mitigate the interference between these two subsystems.
- 4) If two DUEs select the same BPRB, the eNB will compare the channel gain value and allocate the BPRB with the smaller channel gain to the DUE and the other DUE uses the next smallest BPRB. And so on, until each DUE has its own BPRBs to perform D2D transmission.

Summarily, our proposed PRBs allocation scheme is described in **Algorithm 1**. We assume that CUE  $l$  and  $q$  are respectively, a CUE in the IR and a CUE sharing resources with DUE  $m$  outside the IR. DUE  $i$  is another DUE different from DUE  $m$ . We also assume that DUE  $m$  needs  $N_m$  PRBs to finish its transmission.

---

#### **Algorithm 1:** Proposed PRB allocation algorithm for problem (4)

---

##### **%Preparation of interference coordination**

1) Initialize the DUEs, CUEs and PRB vector  $\mathbf{U}^D = (u_1^D, u_2^D, \dots, u_M^D)$ ,  $\mathbf{U}^C = (u_1^C, u_2^C, \dots, u_L^C)$  and  $\mathbf{B} = (b_1, b_2, \dots, b_N)$ .

2) Sort the channel gain of DUE  $m$   $\mathbf{F}_m = (f_{\alpha_{1,m}}^m, f_{\alpha_{2,m}}^m, \dots, f_{\alpha_{N,m}}^m)$  where  $f_{\alpha_{1,m}}^m \leq f_{\alpha_{2,m}}^m \leq \dots \leq f_{\alpha_{N,m}}^m$ . Sort the channel gain of CUE  $l$   $\mathbf{H}_l = (h_{\beta_{1,l}}^l, h_{\beta_{2,l}}^l, \dots, h_{\beta_{N,l}}^l)$ , where  $h_{\beta_{1,l}}^l \geq h_{\beta_{2,l}}^l \geq \dots \geq h_{\beta_{N,l}}^l$ . And  $\{\alpha_{1,m}, \alpha_{2,m}, \dots, \alpha_{N,m}\}$  and  $\{\beta_{1,l}, \beta_{2,l}, \dots, \beta_{N,l}\}$  are the PRB sequence numbers corresponding to DUE  $m$  and CUE  $l$ .

##### **% Proposed PRB and power joint allocation mechanism**

```

n = 1;
for m = 1 to M do
  while n ≤ Nm do
    if αn,i = αn,m
      if fαn,ii < fαn,mm, assign PRB αn,i to DUE i and PRB αn+1,m to DUE m;
    else assign PRB αn,m to DUE m and PRB αn+1,i to DUE i;
    end if
  end if
  if αn,m ≠ βn,l, assign PRB αn,m to DUE m and PRB βn,l to CUE l;
  else assign PRB αn+1,m to DUE m and PRB βn,l to CUE l;
  end if
  n = n + 1;
end while
Allocate BPRBs of DUE m to CUE q;
Remove the allocated PRBs from B, and remove UEs which has obtained all required PRBs from  $U^D$ 
and  $U^C$ .
m = m + 1;
end for

```

---

## 4. Power Allocation Problem

In the following, we develop an approach by which the optimal solution is delimited into at most three vectors which greatly reduces the computational complexity.

### 4.1 Reformulation of the Problem

After using the proposed PRB allocation approach in **Algorithm 1**, the binary PRB assignment variables  $x_{i,n}$  is fixed and the original problem (4) can be reformulated as

$$\begin{aligned}
 \max_{\mathbf{P}^{DUE}, \mathbf{P}^{LTE}} R &= \max_{\mathbf{P}^{DUE}, \mathbf{P}^{LTE}} \sum_{n=1}^N R_n = \max_{\mathbf{P}^{DUE}, \mathbf{P}^{LTE}} \sum_{n=1}^N (\omega_n R_n^{DUE} + (1 - \omega_n) R_n^{LTE}) \\
 &= \max_{\mathbf{P}^{DUE}, \mathbf{P}^{LTE}} B \sum_{n=1}^N \sum_{m=1}^M \omega_n \log_2 \left( 1 + \frac{P_{m,n} h_{m,n} g_{m,n}^{DUE}}{P_{l,n} h_{l,m,n} g_{l,m,n}^{DUE} + \sigma_n^2} \right) \tag{7}
 \end{aligned}$$

$$+ \max_{\mathbf{P}^{DUE}, \mathbf{P}^{LTE}} B \sum_{n=1}^N \sum_{l=1}^L (1 - \omega_n) \log_2 \left( 1 + \frac{P_{l,n} f_{l,n} g_{l,n}^{eNB}}{P_{m,n} f_{m,l,n} g_{m,l,n}^{eNB} + \sigma_n^2} \right)$$

$$\text{s.t.} \quad \gamma_m^{DUE} \geq \gamma_{DUE}^{tgt}, \quad \forall m \tag{C1}$$

$$\gamma_l^{eNB} \geq \gamma_{eNB}^{tgt}, \quad \forall l \tag{C2}$$

$$P_{m,n} \leq P_{\max}^{DUE}, \quad \forall m, n \tag{C3}$$

$$P_{\min}^{CUE} \leq P_{l,n} \leq P_{\max}^{CUE}, \quad \forall l, n \tag{C4}$$

$$P_{l,n} > 0, \quad \forall l, n \tag{C5}$$

where  $\mathbf{P}^{DUE} = (P_1, P_2, \dots, P_M)^T$  and  $\mathbf{P}^{LTE} = (P_1, P_2, \dots, P_L)^T$  are defined as the vectors of the transmission power of DUEs and cellular devices. It is obvious that (7) is a non-convex function which is solvable by the Lagrangian Dual Method. However, it can be observed that for each given PRB, we need to deal with two cubic equations, five linear equations and five



inequalities for five constraints. Moreover, five Lagrangian multipliers need to be determined. Although some methods such as subgradient or ellipsoid can be used to obtain them [20], iterations are still utilized to approximate the optimal solutions and more iterations may happen for a higher optimality accuracy [20]. To avoid such high complexity and decrease signaling overhead thus further to save energy, in the following, we propose an efficient approach by which the optimal solutions can be found by utilizing three lemmas and one theorem. Specifically, we extend our scheme into an imperfect CSI scenario where the exact channel gains between two DUEs and that from CUEs to DUEs are not obtained by an eNB.

## 4.2 Optimal Transmission Power Allocation

**Lemma 1:** The optimal transmission power will not exist when the target SINR for the D2D subsystem and LTE-A networks are set up as  $\gamma_{DUE}^{tgt} > \frac{h_{m,n} g_{m,n}^{DUE}}{h_{l,m,n} g_{m,n}^{DUE}}$  and  $\gamma_{LTE}^{tgt} > \frac{f_{l,n} g_{l,n}^{eNB}}{f_{m,l,n} g_{m,l,n}^{eNB}}$ .

*Proof:* The proof is given in Appendix A.

This lemma guides us to set the target SINR for the hybrid system which is very important to obtain the optimal solutions of the objective function (7).

**Lemma 2:** The optimal solutions of (7) are on the boundary of the feasible region determined by (C1)~(C5).

*Proof:* The proof is provided in Appendix B.

**Lemma 3:** For the feasible region  $\partial\mathcal{P}$  defined by (C1)~(C5), the target weighted sum throughput function on PRB  $n$

$$R_{m,l,n}(P_{m,n}, P_{l,n}) = B \log_2 \left( \left( \frac{1 + \frac{P_{m,n} h_{m,n} g_{m,n}^{DUE}}{P_{l,n} h_{l,m,n} g_{l,m,n}^{DUE} + \sigma_n^2}}{1 + \frac{P_{l,n} f_{l,n} g_{l,n}^{eNB}}{P_{m,n} f_{m,l,n} g_{m,l,n}^{eNB} + \sigma_n^2}} \right)^{\omega_n} \left( 1 + \frac{P_{l,n} f_{l,n} g_{l,n}^{eNB}}{P_{m,n} f_{m,l,n} g_{m,l,n}^{eNB} + \sigma_n^2} \right) \right) \text{ is quasiconcave.}$$

*Proof:* This proof is described in Appendix C in detail.

With Lemma 1, 2 and 3, we present the main result on optimal power allocation below.

**Theorem 1:** The optimal power vector achieving target weighted sum throughput lies in the following set

$$P_{opt} = \begin{cases} (P_{\max}^{CUE}, P_{m,n}^1), (P_{\max}^{CUE}, P_{m,n}^2), & \gamma_{DUE}^{tgt} < \Lambda \text{ and } \gamma_{eNB}^{tgt} > \Gamma \\ (P_{\max}^{CUE}, P_{m,n}^1), (P_{\max}^{CUE}, P_{\max}^{DUE}), (P_{l,n}^2, P_{\max}^{DUE}), & \gamma_{DUE}^{tgt} < \Lambda \text{ and } \gamma_{eNB}^{tgt} \leq \Gamma \\ (P_{l,n}^1, P_{\max}^{DUE}), (P_{l,n}^2, P_{\max}^{DUE}), & \gamma_{DUE}^{tgt} \geq \Lambda \text{ and } \gamma_{eNB}^{tgt} \leq \Gamma \end{cases}$$

where

$$P_{m,n}^1 = \frac{h_{l,m,n} g_{l,m,n}^{DUE} \gamma_{DUE}^{tgt}}{h_{m,n} g_{m,n}^{DUE}} P_{\max}^{CUE} + \frac{\gamma_{DUE}^{tgt} \sigma_n^2}{h_{m,n} g_{m,n}^{DUE}}, P_{m,n}^2 = \frac{f_{l,n} g_{l,n}^{eNB}}{f_{m,l,n} g_{m,l,n}^{eNB}} P_{\max}^{CUE} - \frac{\gamma_{eNB}^{tgt} \sigma_n^2}{f_{m,l,n} g_{m,l,n}^{eNB}},$$

$$P_{l,n}^1 = \frac{h_{m,n} g_{m,n}^{DUE}}{h_{l,m,n} g_{l,m,n}^{DUE}} P_{\max}^{DUE} - \frac{\gamma_{DUE}^{tgt} \sigma_n^2}{h_{l,m,n} g_{l,m,n}^{DUE}}, P_{l,n}^2 = \frac{f_{m,l,n} g_{m,l,n}^{eNB} \gamma_{eNB}^{tgt}}{f_{l,n} g_{l,n}^{eNB}} P_{\max}^{DUE} + \frac{\gamma_{eNB}^{tgt} \sigma_n^2}{f_{l,n} g_{l,n}^{eNB}},$$

$$\Lambda = \frac{P_{\max}^{DUE} h_{m,n} g_{m,n}^{DUE}}{P_{\max}^{CUE} h_{l,m,n} g_{l,m,n}^{DUE} + \sigma_n^2}, \text{ and } \Gamma = \frac{P_{\max}^{CUE} f_{l,n} g_{l,n}^{eNB}}{P_{\max}^{DUE} f_{m,l,n} g_{m,l,n}^{eNB} + \sigma_n^2}.$$

*Proof:* Based on the above three lemmas, the optima  $(P_{m,n}^*, P_{l,n}^*)$  occurs on the endpoint of the boundary of the feasible region. Furthermore, the objective function is monotonically increasing on  $l_4$  and  $l_5$ , the intersection of these two lines and the endpoints on the  $l_2$  are excluded. Thus completes the proof.

### 4.3 Power Allocation for Imperfect CSI

The above **Theorem 1** gives an optimal power transmission solution which depends on the perfect channel gains between CUEs and DUEs and that from UEs to the eNB. In a practical LTE system, it is reasonable for the eNB to obtain the CSI from the UEs to itself by detecting UL RSs. However, the distributed nature of the D2D communication may increase the additional signaling overhead for the eNB to obtain CSI between two DUEs and that from one CUE to a victim DUE. As such, we use statistical estimates of CSI to set the transmitted power, that is to say, let  $\overline{h_{m,n} g_{m,n}^{DUE}} = E(h_{m,n} g_{m,n}^{DUE})$  and  $\overline{h_{l,m,n} g_{l,m,n}^{DUE}} = E(h_{l,m,n} g_{l,m,n}^{DUE})$ . This is a practical choice and equivalent to power controlling over the pathloss and ignoring the fast fading effects [13] and this gives a feasible method for the eNB to perform power allocation with minimal overhead. Therefore, we get **Theorem 2** in the imperfect CSI scenario as follows.

**Theorem 2:** The optimal power vector achieving target weighted sum throughput under the imperfect CSI scenario lies in the following set

$$P_{opt} = \begin{cases} \left( P_{max}^{CUE}, \min(P_{m,n}^1, P_{m,n}^{req}) \right), \left( P_{max}^{CUE}, P_{m,n}^2 \right), & \gamma_{DUE}^{tgt} < \Lambda \text{ and } \gamma_{eNB}^{tgt} > \Gamma \\ \left( P_{max}^{CUE}, \min(P_{m,n}^1, P_{m,n}^{req}) \right), \left( P_{max}^{CUE}, P_{max}^{DUE} \right), \left( P_{l,n}^2, P_{max}^{DUE} \right), & \gamma_{DUE}^{tgt} < \Lambda \text{ and } \gamma_{eNB}^{tgt} \leq \Gamma \\ \left( \max(P_{l,n}^1, P_{min}^{CUE}), P_{max}^{DUE} \right), \left( P_{l,n}^2, P_{max}^{DUE} \right), & \gamma_{DUE}^{tgt} \geq \Lambda \text{ and } \gamma_{eNB}^{tgt} \leq \Gamma \end{cases}$$

where

$$\begin{aligned} P_{m,n}^1 &= \frac{\overline{h_{l,m,n} g_{l,m,n}^{DUE}} \gamma_{DUE}^{tgt}}{h_{m,n} g_{m,n}^{DUE}} P_{max}^{CUE} + \frac{\gamma_{DUE}^{tgt} \sigma_n^2}{h_{m,n} g_{m,n}^{DUE}}, P_{m,n}^2 = \frac{f_{l,n} g_{l,n}^{eNB}}{f_{m,l,n} g_{m,l,n}^{eNB}} P_{max}^{CUE} - \frac{\gamma_{eNB}^{tgt} \sigma_n^2}{f_{m,l,n} g_{m,l,n}^{eNB}}, \\ P_{l,n}^1 &= \frac{\overline{h_{m,n} g_{m,n}^{DUE}}}{h_{l,m,n} g_{l,m,n}^{DUE}} P_{max}^{DUE} - \frac{\gamma_{DUE}^{tgt} \sigma_n^2}{h_{l,m,n} g_{l,m,n}^{DUE}}, P_{l,n}^2 = \frac{f_{m,l,n} g_{m,l,n}^{eNB} \gamma_{eNB}^{tgt}}{f_{l,n} g_{l,n}^{eNB}} P_{max}^{DUE} + \frac{\gamma_{eNB}^{tgt} \sigma_n^2}{f_{l,n} g_{l,n}^{eNB}}, \\ P_{m,n}^{req} &= \frac{f_{l,n} g_{l,n}^{eNB} P_{max}^{CUE}}{f_{m,l,n} g_{m,l,n}^{eNB} \gamma_{eNB}^{tgt}} - \frac{\sigma_n^2}{f_{m,l,n} g_{m,l,n}^{eNB}}, \Lambda = \frac{P_{max}^{DUE} \overline{h_{m,n} g_{m,n}^{DUE}}}{P_{max}^{CUE} \overline{h_{l,m,n} g_{l,m,n}^{DUE}} + \sigma_n^2}, \text{ and } \Gamma = \frac{P_{max}^{CUE} f_{l,n} g_{l,n}^{eNB}}{P_{max}^{DUE} f_{m,l,n} g_{m,l,n}^{eNB} + \sigma_n^2}. \end{aligned}$$

Please refer to Appendix D for the proof in detail.

We should note that although the D2D performance is slightly damaged in the imperfect CSI case, we can adjust the weight  $\omega_n$  to compensate the decreased throughput.

### 4.4 Computational Complexity and Overhead Analysis

From the above analyses we observe that the original MINLP is an NP-hard problem whose normal solution is exhaustive search. The lower computational complexity can be obtained by using the proposed power allocation scheme. To better understand our scheme, in the following the computational complexity of our method and traditional LDO are analyzed.

Suppose that the same PRB selection strategy is adopted for which no additional overhead is

incurred since channel estimation is requisite for existing LTE systems. Our power optimization algorithm needs to solve only two linear equations on each given PRB such that the complexity of our proposed scheme is  $O(2N)$  for allocating  $N$  PRBs. Compared with classical LDO with KKT conditions which needs to deal with two cubic equations, five linear equations and five inequalities for each given PRB, our approach has much lower complexity. Specifically, for the LDO, five Lagrange multipliers need to be determined by using some iterative algorithms. Suppose the subgradient method is utilized to obtain required  $\delta$ -optimality, then the needed iteration number is on the order of  $O(1/\delta^2)$  [20]. Consequently, the required computational complexity for LDO can be expressed as  $O(I \cdot D(\mathfrak{S}) \cdot N \cdot (1/\delta^2))$  for  $N$  subchannels, where  $I$  is the required subgradient updates to approach the  $\delta$ -optimality and  $D$  denotes the dimension of LDO set  $\mathfrak{S}$ . Therefore, the proposed scheme is computationally efficient in finding optimal solutions compared with the classical LDO.

From the overhead perspective, we know that D2D users are still in the control of the eNB which means that it is natural that the eNB obtains the perfect CSI from the CUEs and DUEs to itself like a normal LTE system. Thus, our developed PRBs assignment scheme does not incur additional signaling overhead into the current LTE-A systems. Although global CSI is needed to obtain perfect transmission power by using *Theorem 1*, we obtain *Theorem 2* for the imperfect CSI scenario to reduce the signaling overhead produced by sending CSI between two D2D UEs and that from a CUE to the victim DUE. The following simulations prove satisfying performance still can be obtained by using the proposed *Theorem 2*.

Furthermore, we define  $Q[\cdot]_x$  as an  $x$  bit quantizer to quantize the input variable and thus the total amount of signaling overhead of the proposed method can be calculated as

$$\underbrace{M \times N_m \times Q[h_{m,n} g_{m,n}^{DUE}]_x}_{\text{CSI feedback overhead between two DUEs}} + \underbrace{L^* \times N^* \times Q[h_{l,m,n} g_{l,m,n}^{DUE}]_x}_{\text{CSI feedback overhead between CUEs and victim DUEs}} \\ + \underbrace{L \times N_l \times Q[PRB_{l,n}^*]_x + M \times N_m \times Q[PRB_{m,l,n}^*]_x}_{\text{eNB feeds back determined PRBs}} + \underbrace{L \times N_l \times Q[P_{l,n}]_x + M \times N_m \times Q[P_{m,n}]_x}_{\text{eNB feeds back used power}}$$

where  $L^*$  and  $N^*$  represent the number of CUEs which interfere with the approximate DUEs on  $N^*$  PRBs.  $N_l$  and  $N_m$  denote the used PRBs for each CUE and DUE.  $PRB_{l,n}^*$  and  $PRB_{m,l,n}^*$  are selected PRBs for a CUE and a DUE respectively.

#### 4.5 Joint PRB and Power Allocation

To provide a complete understanding of the proposed joint PRB and power allocation scheme, we devise the protocol in a practical LTE-A system which is shown in **Algorithm 2**.

---

**Algorithm 2:** Proposed algorithm for jointly allocating transmission power and PRBs

---

**%Preparation of interference coordination**

- 1) The eNB obtains all CSI and identifies the SPRBs and BPRBs for each UE.
- 2) The eNB obtains the IR information for each DUE.
- 3) For D2D transmission, the handshaking procedure described in Section 3 is realized.

**% Proposed PRB allocation scheme**

- 4) The eNB allocates the PRBs according to the **Algorithm 1** which is described in Section 3.

**% Proposed power allocation algorithm**

- 5) Initialize  $\gamma_{NB}^{tgt}$  and  $\gamma_{DUE}^{tgt}$ , calculate  $\Lambda$  and  $\Gamma$ .
- 6) **If** perfect CSI can be obtained by the eNB

- ```

then Theorem 1 is used for the optimal power vector
for  $i = 1 \rightarrow$  the number of the vectors in this group do
    Substitute  $(P_{m,n}^i, P_{l,n}^i)$  into the target objective function of (7).
    if  $(P_{m,n}^i, P_{l,n}^i) = \max_{\mathbf{p}^{DUE}, \mathbf{p}^{LTE}} R_n$ 
        then  $(P_{m,n}^*, P_{l,n}^*) = (P_{m,n}^i, P_{l,n}^i)$ 
    end if
end for
else Theorem 2 is used for the optimal power vector
for  $i = 1 \rightarrow$  the number of the vectors in this group do
    Substitute  $(\overline{P}_{m,n}^i, \overline{P}_{l,n}^i)$  into the target objective function of (7).
    if  $(\overline{P}_{m,n}^i, \overline{P}_{l,n}^i) = \max_{\mathbf{p}^{DUE}, \mathbf{p}^{LTE}} R_n$ 
        then  $(P_{m,n}^*, P_{l,n}^*) = (\overline{P}_{m,n}^i, \overline{P}_{l,n}^i)$ 
    end if
end for
end if

```
- 7) The eNB allocates the transmission power for the CUE and the DUE on PRB  $n$ .
  - 8) The CUE and the DUE which share the same resources perform transmission on the assigned PRBs according to the allocated transmission power.

## 5. Simulation and Performance Analysis

In this section, simulation results are provided to evaluate the performance of our proposed scheme when sharing UL spectrums in a LTE-A system.

### 5.1 Simulation Parameters

We consider a cell with a radius of 300m and cellular users are dropped uniformly whereas D2D users are distributed in a randomly placed cluster with a maximal radius of 30m through the cell. The used system bandwidth is 20MHz, i.e., 100 PRBs altogether. The maximal power constraint for the CUE is 23dBm with respect to that of a DUE is 13dBm to favor the short distance between two D2D users. The small-scale fading is modeled by a multi-path Rayleigh fading process and we also set  $\gamma_{LTE}^{tgt} = \gamma_{DUE}^{tgt} = 20\text{dB}$ . In a practical LTE system,  $\omega_n$  is given by the operator to scale the sum throughput and fairness, in our simulations  $\omega_n \in [0, 1]$ . The detailed parameters are set up according to [21] and are presented in **Table 1**.

**Table 1.** Parameters for simulation

|                            |             |
|----------------------------|-------------|
| Distance of two D2D UEs    | 10 m~60m    |
| Noise Power Density        | -174 dBm/Hz |
| Noise figure               | 5 dB        |
| Number of active CUEs      | 20~50       |
| Number of active D2D pairs | 6~41        |
| IR distance                | 10m~50m     |
| Weight of D2D users        | 0.4~0.7     |

|                                   |                                                                                            |
|-----------------------------------|--------------------------------------------------------------------------------------------|
| Cellular link pathloss (PL) model | $PL=128.1+37.6*\log_{10}(R)$ , R is the transmitter-receiver separation in kilometers [22] |
| D2D link pathloss model           | $PL=127+30*\log_{10}(R)$ , R is the transmitter-receiver separation in kilometers [22]     |
| system bandwidth                  | 20MHz, i.e., 100PRBs                                                                       |
| RB bandwidth                      | 180 kHz                                                                                    |
| Carrier frequency                 | 2000 MHz                                                                                   |

## 5.2 System Weighted Throughput and Power Efficiency for Perfect CSI

Fig. 2, 3 and 4 firstly present the system weighted sum throughput, D2D subsystem throughput and LTE-A system throughput separately when different algorithms are utilized. In our work, five algorithms are considered. *Algorithm 1* is our proposed PRB and power joint allocation. *Algorithm 2* uses the proposed PRB allocation mechanism but sets up the power according to the LTE specification [23]. *Algorithm 3* randomly allocates PRBs but uses the maximum transmission power and *Algorithm 4* selects PRB randomly and sets up power by [23]. To compare with the existing research, we also simulate the scheme according to [7] and denote it as *Algorithm 5*. The used benchmark is the perfect scenario that PRBs are allocated completely orthogonally between DUEs and CUEs with maximum transmission power. In our simulation, the used D2D distance and IR distance are respectively 10m and 30m. The adopted weights for the D2D subsystem and LTE-A network are 0.4 and 0.6 to give the licensed cellular users a higher priority. We fix the active CUE number as 50 and change active DUE pairs from 6 to 41.

Three observations can be made from Fig. 2, 3 and 4. First of all, our method outperforms the other four algorithms when system weighted sum throughput, D2D subsystem throughput and LTE-A system throughput are evaluated. This result proves the effectiveness of our method. Secondly, with the increase of the DUE number, our scheme obtains a larger gain. This is due to the fact that more interference is incurred by D2D users and such interference can be effectively suppressed by appropriately allocating PRBs by using our mechanism. Finally, the performance of the cellular subsystem is warranted by using our devised scheme. To constrain the target QoS of the LTE-A network, its performance will not become worse with the increase of D2D users. We should note that the developed scheme in [7] aims to maximize the throughput of the D2D subsystem instead of the system sum throughput. Consequently, the system sum throughput and cellular system throughput reduce with the increase of D2D users in spite of the D2D subsystem throughput increases.

To study the power efficiency (PE), we define  $PE = \text{sum throughput} / \text{sum consumed power}$  and show the PE of different algorithms in Fig. 5. From this figure we may conclude that our proposed PRB allocation scheme is energy efficient. For example, by comparing the simulations of Algorithm 2 and Algorithm 4, we can see that the larger PE can be obtained by performing the proposed PRB allocation strategy than using the maximal transmission power with random PRB allocation. From this point of view, our developed method is an energy efficient strategy and it may save transmission power of terminals. This is very important by considering the fact that the mobile terminals are battery-constrained devices.

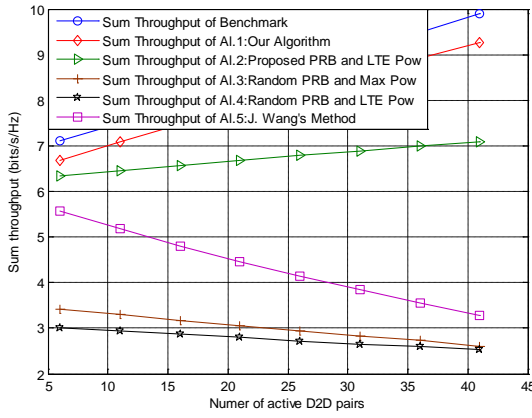


Fig. 2. System sum throughput versus D2D pairs for different algorithms.

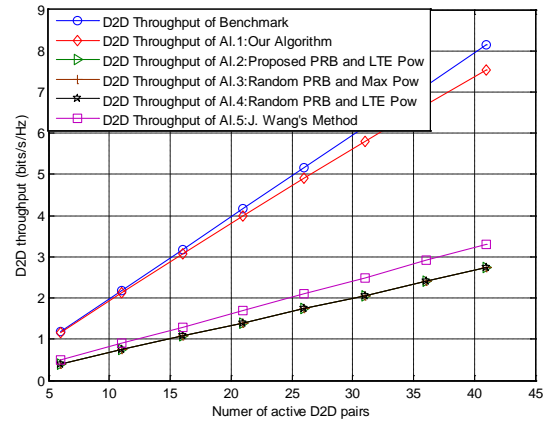


Fig. 3. D2D subsystem throughput versus D2D pairs for different algorithms.

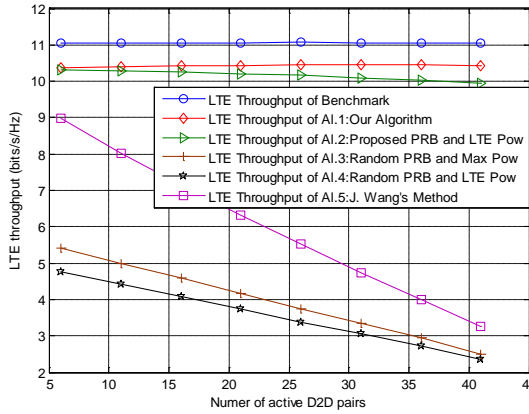


Fig. 4. LTE subsystem throughput versus D2D pairs for different algorithms.

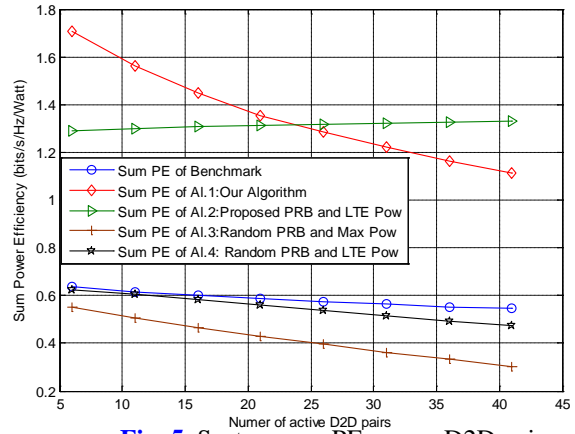


Fig. 5. System sum PE versus D2D pairs for different algorithms.

### 5.3 System Weighted Sum Throughput for Different Parameters for Perfect CSI

We further investigate our approach when considering different parameters in a perfect CSI scenario and show the results in Fig. 6, 7 and 8. Fig. 6 presents the impact of the interference region when it changes from 10m to 30m. The adopted weights for the D2D subsystem and cellular network are 0.4 and 0.6 separately. We also fix the distance between two D2D users to be 10m and consider a perfect CSI scenario. From this figure we observe that a slight difference exists for different IR when the number of D2D users is small. However, a higher gain is obtained by selecting a large IR with the increase of D2D users. This is because that a larger IR leads to more CUEs to be taken into account as disturbers and thus further requires more orthogonal resources to be used between these two subsystems. As a result, better performance will be obtained by adopting a large IR. Nevertheless, more orthogonal resources may decrease the spectrum efficiency. Therefore, a tradeoff should be considered to obtain the satisfying sum throughput and high spectrum efficiency.

We also change the distance between two D2D users and weights of a DUE and a CUE to evaluate our algorithm and show the results in Fig. 7. The IR is set up as 30m and a perfect CSI scenario is considered. Fig. 7 indicates that the system sum throughput will reduce with the

increase of the distance between two D2D users and this is an intuitive result. We also observe that better performance is obtained when we give the licensed CUEs a higher weight whereas this gain is gradually negligible with the increase of D2D users.

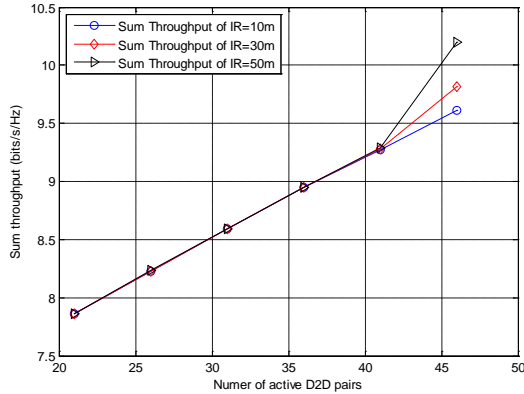


**Fig. 6** System sum throughput versus D2D pairs for different IR distance.

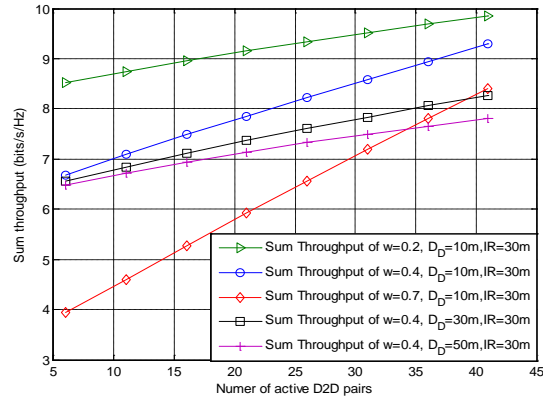


**Fig. 7.** System sum throughput versus D2D pairs for different D2D distance and weights.

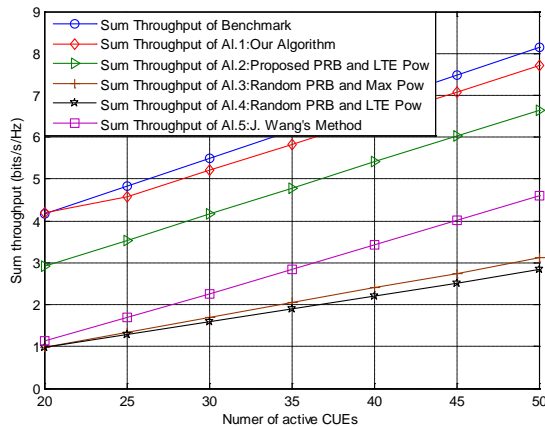


**Fig. 8.** System sum throughput versus CUEs numbers for different algorithms.

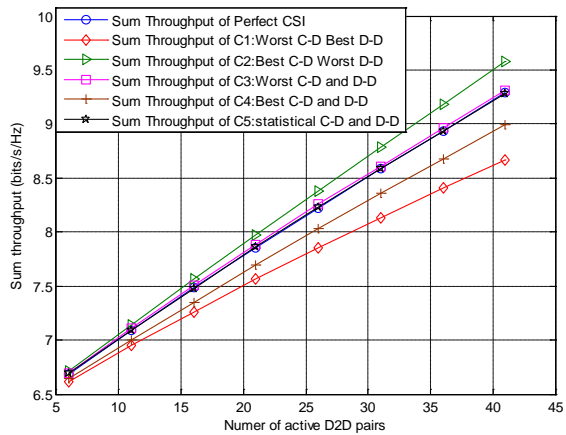


**Fig. 9.** System sum throughput versus DUE pairs in an imperfect CSI scenario.

**Fig. 8** illustrates the impact of CUE numbers by fixing the DUE number to be 19 and changing CUE numbers from 20 to 50. From this figure we conclude that our method still can obtain better performance than other four algorithms.

#### 5.4 System Weighted Sum Throughput for Imperfect CSI

To get insight of the proposed mechanism in an imperfect CSI scenario, we plot weighted system sum throughput in the function of the number of D2D pairs for five cases in **Fig. 9**. The used weights are 0.4 and 0.6 respectively for DUEs and CUEs. And the adopted IR and D2D distance are 30m and 10m, separately.

In *Case 1*, the worst channel gains between a CUE and a victim DUE (i.e.  $h_{l,m,n} g_{l,m,n}^{DUE}$ ) are adopted but the best channel gains between two D2D users (i.e.  $h_{m,n} g_{m,n}^{DUE}$ ) are used. In *Case 2*,

we utilize the best  $h_{l,m,n}g_{l,m,n}^{DUE}$  but the worst  $h_{m,n}g_{m,n}^{DUE}$ . For *Case 3*,  $h_{l,m,n}g_{l,m,n}^{DUE}$  and  $h_{m,n}g_{m,n}^{DUE}$  are both the worst values. On the contrary, *Case 4* uses the best  $h_{l,m,n}g_{l,m,n}^{DUE}$  and  $h_{m,n}g_{m,n}^{DUE}$ . In *Case 5*, we use statistical estimates of  $h_{l,m,n}g_{l,m,n}^{DUE}$  and  $h_{m,n}g_{m,n}^{DUE}$  which are averaged results over a period. From **Fig. 9** we firstly demonstrate that to use the statistical estimates of CSI (namely *Case 5*) is feasible which is very close to the result in a perfect CSI scenario. We also observe that to use the best  $h_{l,m,n}g_{l,m,n}^{DUE}$  but the worst  $h_{m,n}g_{m,n}^{DUE}$  (namely *Case 2*) actually gives the upper bound of our algorithm whilst the worst  $h_{l,m,n}g_{l,m,n}^{DUE}$  and best  $h_{m,n}g_{m,n}^{DUE}$  (namely *Case 1*) approach to the lower bound of our scheme.

## 6. Conclusions

In this work, we studied the PRBs and transmission power joint allocation in a D2D underlaying LTE-A network when sharing UL spectrums. To maximize the weighted sum throughput, we proposed an energy efficient PRBs allocation strategy by which not only the interference suffered by the LTE-A devices but also to the D2D users are mitigated effectively. Furthermore, the optimal transmission power is obtained by using a low-complexity algorithm and the optimal power vector is delimited in at most three power vectors. Specifically, we extend our study to an imperfect CSI scenario. Simulations show that the proposed resource allocation scheme improves system performance significantly compared with the other existing methods.

## Appendix

### A. Proof of Lemma 1

From (C1) and (C2) in (7) we have

$$P_{m,n} \left( 1 - \frac{h_{l,m,n}g_{m,n}^{DUE}}{h_{m,n}g_{m,n}^{DUE}} \gamma_{DUE}^{tgt} \times \frac{f_{m,l,n}g_{m,l,n}^{eNB}}{f_{l,n}g_{l,n}^{eNB}} \gamma_{eNB}^{tgt} \right) = \frac{\sigma_n^2}{h_{m,n}g_{m,n}^{DUE}} \left( \gamma_{DUE}^{tgt} + \frac{h_{l,m,n}g_{m,n}^{DUE}}{f_{l,n}g_{l,n}^{eNB}} \gamma_{DUE}^{tgt} \gamma_{eNB}^{tgt} \right) \quad (8)$$

which requires  $\frac{h_{l,m,n}g_{m,n}^{DUE}}{h_{m,n}g_{m,n}^{DUE}} \gamma_{DUE}^{tgt} \times \frac{f_{m,l,n}g_{m,l,n}^{eNB}}{f_{l,n}g_{l,n}^{eNB}} \gamma_{eNB}^{tgt} < 1$ . Thus when  $\frac{h_{l,m,n}g_{m,n}^{DUE}}{h_{m,n}g_{m,n}^{DUE}} \gamma_{DUE}^{tgt} > 1$

and  $\frac{f_{m,l,n}g_{m,l,n}^{eNB}}{f_{l,n}g_{l,n}^{eNB}} \gamma_{eNB}^{tgt} > 1$  there is no solution for the original problem such that *Lemma 1* holds.

### B. Proof of Lemma 2

As illustrated in **Fig. 10**, let  $\Psi$  be the area determined by (C1)~(C5) in (7). Note that by properly selecting the parameters of  $P_{max}^{DUE}, P_{max}^{CUE}, P_{min}^{CUE}, \gamma_{DUE}^{tgt}$  and  $\gamma_{eNB}^{tgt}$  and guaranteeing *Lemma 1* not to happen,  $\Psi$  can be a closed convex polygon. We also should note that the feasible area of (7) has several possibilities according to the real values, we just show one possibility in **Fig. 10**.

We further define  $\partial\Psi$  is the boundary of  $\Psi$  and  $\Psi' = \Psi - \partial\Psi$ . Assume  $P^* = (P_{m,n}^*, P_{l,n}^*)$  be the optimal power of a DUE  $m$  and the  $l$ th cellular device operating on PRB  $n$  and  $P^* \in \Psi'$ , so we



have  $P^*(P_{m,n}^*, P_{l,n}^*) = \max_{P_{m,n}^*, P_{l,n}^*} R_{l,m,n}^* = \max_{P_{m,n}^*, P_{l,n}^*} (\omega_n R_n^{DUE} + (1-\omega_n) R_n^{LTE})$ . Thus, there always exists a line across the origin and  $P^*$  with the slope  $\tau = P_{l,n}^*/P_{m,n}^* > 0$  and this line intersects  $\partial\mathcal{P}$  at the point  $P^\dagger = (P_{m,n}^\dagger, P_{l,n}^\dagger)$ . It is obvious that  $P_{m,n}^\dagger > P_{m,n}^*$  and we let  $P_{m,n}^\dagger = \alpha P_{m,n}^*$  with  $\alpha > 1$ . Consequently, we have  $P_{l,n}^\dagger = \alpha P_{l,n}^*$  considering the fact that  $\tau = (P_{m,n}^\dagger - P_{m,n}^*) / (P_{l,n}^\dagger - P_{l,n}^*)$ . Substituting  $P^* = (P_{m,n}^*, P_{l,n}^*)$  and  $P^\dagger = (P_{m,n}^\dagger, P_{l,n}^\dagger) = (\alpha P_{m,n}^*, \alpha P_{l,n}^*)$  into  $R_{m,l,n}^\dagger(P_{m,n}^\dagger, P_{l,n}^\dagger) = B\omega_n \log_2(1 + \gamma_{m,n}^{DUE}) + B(1-\omega_n) \log_2(1 + \gamma_{l,n}^{eNB})$ , we get

$$\begin{aligned}
R_{m,l,n}^\dagger(P_{m,n}^\dagger, P_{l,n}^\dagger) &= B \left( \log_2(1 + \gamma_{m,n}^{DUE})^{\omega_n} \times \log_2(1 + \gamma_{l,n}^{eNB})^{-\omega_n} \times \log_2(1 + \gamma_{l,n}^{eNB}) \right) \\
&= B \left( \log_2 \left( 1 + \frac{P_{m,n}^\dagger h_{m,n} g_{m,n}^{DUE}}{P_{l,n}^\dagger h_{l,m,n} g_{l,m,n}^{DUE} + \sigma_n^2} \right)^{\omega_n} \log_2 \left( 1 + \frac{P_{l,n}^\dagger f_{l,n} g_{l,n}^{eNB}}{P_{m,n}^\dagger f_{m,l,n} g_{m,l,n}^{eNB} + \sigma_n^2} \right)^{-\omega_n} \log_2 \left( 1 + \frac{P_{l,n}^\dagger f_{l,n} g_{l,n}^{eNB}}{P_{m,n}^\dagger f_{m,l,n} g_{m,l,n}^{eNB} + \sigma_n^2} \right) \right) \\
&= B \left( \log_2 \left( 1 + \frac{P_{m,n}^* h_{m,n} g_{m,n}^{DUE}}{P_{l,n}^* h_{l,m,n} g_{l,m,n}^{DUE} + \frac{\sigma_n^2}{\alpha}} \right)^{\omega_n} \log_2 \left( 1 + \frac{P_{l,n}^* f_{l,n} g_{l,n}^{eNB}}{P_{m,n}^* f_{m,l,n} g_{m,l,n}^{eNB} + \frac{\sigma_n^2}{\alpha}} \right)^{-\omega_n} \log_2 \left( 1 + \frac{P_{l,n}^* f_{l,n} g_{l,n}^{eNB}}{P_{m,n}^* f_{m,l,n} g_{m,l,n}^{eNB} + \frac{\sigma_n^2}{\alpha}} \right) \right) \\
&> B \left( \log_2 \left( 1 + \frac{P_{m,n}^* h_{m,n} g_{m,n}^{DUE}}{P_{l,n}^* h_{l,m,n} g_{l,m,n}^{DUE} + \sigma_n^2} \right)^{\omega_n} \log_2 \left( 1 + \frac{P_{l,n}^* f_{l,n} g_{l,n}^{eNB}}{P_{m,n}^* f_{m,l,n} g_{m,l,n}^{eNB} + \sigma_n^2} \right)^{-\omega_n} \log_2 \left( 1 + \frac{P_{l,n}^* f_{l,n} g_{l,n}^{eNB}}{P_{m,n}^* f_{m,l,n} g_{m,l,n}^{eNB} + \sigma_n^2} \right) \right) \\
&= R_{m,l,n}^*(P_{m,n}^*, P_{l,n}^*).
\end{aligned}$$

The last inequality uses the monotonical increase of logarithm when the base larger than 1 and the fact that  $\alpha > 1$ . Thus we have  $R_{m,l,n}^\dagger(P_{m,n}^\dagger, P_{l,n}^\dagger) > R_{m,l,n}^*(P_{m,n}^*, P_{l,n}^*)$  and this contradicts the assumption that  $P^* = (P_{m,n}^*, P_{l,n}^*)$  is the optimal solution. As the result, Lemma 2 holds.

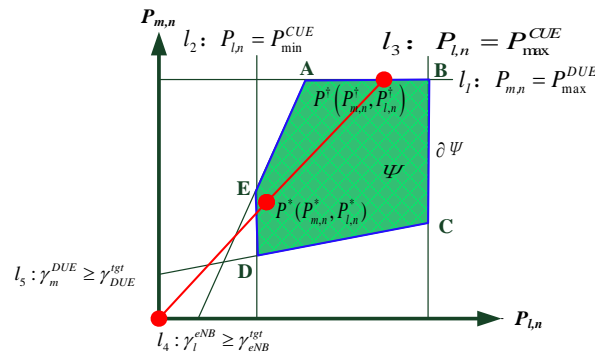


Fig. 10. Illustration of the feasible region for the target function (7).

### C. Proof of Lemma 3

Using monotonicity of logarithm, maximizing  $R_{m,l,n}$  is to maximize

$$Q(P_{m,n}, P_{l,n}) = \left( \frac{1 + \frac{P_{m,n} h_{m,n} g_{m,n}^{DUE}}{P_{l,n} h_{l,m,n} g_{l,m,n}^{DUE} + \sigma_n^2}}{1 + \frac{P_{l,n} f_{l,n} g_{l,n}^{eNB}}{P_{m,n} f_{m,l,n} g_{m,l,n}^{eNB} + \sigma_n^2}} \right)^{\omega_n} \left( 1 + \frac{P_{l,n} f_{l,n} g_{l,n}^{eNB}}{P_{m,n} f_{m,l,n} g_{m,l,n}^{eNB} + \sigma_n^2} \right). \quad (9)$$

According to Lemma 2, we have known that the optimal solution to the problem (7) is obtained at the boundary of the feasible region  $\Psi$  which concludes five lines at most. Consequently, to prove Lemma 3 is to prove  $Q$  function is quasiconcave on these five lines as shown in Fig. 10.

1) We firstly consider  $l_1: P_{m,n} = P_{max}^{CUE}$  by differentiating  $Q(P_{max}^{CUE}, P_{l,n})$  with respect to  $P_{l,n}$ . We

obtain 
$$\frac{\partial Q}{\partial P_{l,n}} = -\omega_n A^{\omega_n - 1} \left( \frac{P_{max}^{CUE} h_{l,m,n} g_{l,m,n}^{DUE} h_{m,n} g_{m,n}^{DUE}}{(P_{l,n} h_{l,m,n} g_{l,m,n}^{DUE} + \sigma_n^2)^2} + \frac{B \left( 1 + \frac{P_{max}^{CUE} h_{m,n} g_{m,n}^{DUE}}{P_{l,n} h_{l,m,n} g_{l,m,n}^{DUE} + \sigma_n^2} \right)}{C} \right) + A^{\omega_n} B, \quad \text{where}$$

$$A = \frac{1 + \frac{P_{max}^{CUE} h_{m,n} g_{m,n}^{DUE}}{P_{l,n} h_{l,m,n} g_{l,m,n}^{DUE} + \sigma_n^2}}{1 + \frac{P_{l,n} f_{l,n} g_{l,n}^{eNB}}{P_{max}^{CUE} f_{m,l,n} g_{m,l,n}^{eNB} + \sigma_n^2}}, \quad B = \frac{f_{l,n} g_{l,n}^{eNB}}{P_{max}^{CUE} f_{m,l,n} g_{m,l,n}^{eNB} + \sigma_n^2} \quad \text{and} \quad C = 1 + \frac{P_{l,n} f_{l,n} g_{l,n}^{eNB}}{P_{max}^{CUE} f_{m,l,n} g_{m,l,n}^{eNB} + \sigma_n^2}.$$

Therefore:

a) If  $\frac{\partial Q}{\partial P_{l,n}} > 0$ , we have  $Q(P_{m,n}, P_{l,n})$  is monotonocally increasing on  $l_1$ . Therefore the maximum

is attained at the endpoint of  $l_1$ .

b) If  $\frac{\partial Q}{\partial P_{l,n}} < 0$ , we need to check the second-order derivative of  $Q$  with respect to  $P_{l,n}$ , namely

$$\frac{\partial^2 Q}{\partial P_{l,n}^2}, \text{ we can easily observe that } \frac{\partial^2 Q}{\partial P_{l,n}^2} < 0 \text{ due to } \frac{\partial A}{\partial P_{l,n}} < 0 \text{ and } P_{l,n} \text{ is in the denominator which}$$

results to the negative value. Thus it is proved that  $Q(P_{m,n}, P_{l,n})$  is concave with respect to  $P_{l,n}$  on  $l_1$  and the optimal value is the maximum.

2) Similarly, we can obtain same conclusions on  $l_2: P_{l,n} = P_{min}^{CUE}$  and  $l_3: P_{l,n} = P_{max}^{CUE}$ .

3) Then we consider  $l_4: \gamma_{eNB}^{tgt} = \frac{P_{l,n} f_{l,n} g_{l,n}^{eNB}}{P_{m,n} f_{m,l,n} g_{m,l,n}^{eNB} + \sigma_n^2}$ . Substitute the expression of

$$P_{m,n} = \frac{P_{l,n} f_{l,n} g_{l,n}^{eNB}}{\gamma_{eNB}^{tgt} f_{m,l,n} g_{m,l,n}^{eNB}} - \frac{\sigma_n^2}{f_{m,l,n} g_{m,l,n}^{eNB}}$$

into the  $Q$  expression, we have

$$Q(P_{m,n}, P_{l,n}) = \left( 1 + \frac{\frac{h_{m,n} g_{m,n}^{DUE} f_{l,n} g_{l,n}^{eNB}}{f_{m,l,n} g_{m,l,n}^{eNB} \gamma_{eNB}^{tgt}} P_{l,n} - \frac{h_{m,n} g_{m,n}^{DUE} \sigma_n^2}{f_{m,l,n} g_{m,l,n}^{eNB}}}{P_{l,n} h_{l,m,n} g_{l,m,n}^{DUE} + \sigma_n^2} \right)^{\omega_n} \left( 1 + \gamma_{eNB}^{tgt} \right), \quad (10)$$

then the first derivative with respect to  $P_{l,n}$  can be obtained as

$$\frac{dQ}{dP_{l,n}} = \omega_n D^{\omega_n - 1} \frac{h_{m,n} g_{m,n}^{DUE} \sigma_n^2 (f_{l,n} g_{l,n}^{eNB} + \gamma_{eNB}^{tgt})}{(P_{l,n} h_{l,m,n} g_{l,m,n}^{DUE} + \sigma_n^2)^2 f_{m,l,n} g_{m,l,n}^{eNB} \gamma_{eNB}^{tgt}}, \quad (11)$$

where  $D = \frac{1 + \frac{h_{m,n} g_{m,n}^{DUE} f_{l,n} g_{l,n}^{eNB}}{f_{m,l,n} g_{m,l,n}^{eNB} \gamma_{eNB}^{tgt}} P_{l,n} - \frac{h_{m,n} g_{m,n}^{DUE} \sigma_n^2}{f_{m,l,n} g_{m,l,n}^{eNB}}}{P_{l,n} h_{l,m,n} g_{l,m,n}^{DUE} + \sigma_n^2}}$ . It is obvious that  $\frac{dQ}{dP_{l,n}} > 0$  which means

that  $Q(P_{m,n}, P_{l,n})$  is monotonically increasing on  $l_4$ .

4) Following the same procedure, taking the first derivative with respect to  $P_{l,n}$  on  $l_5$ :

$\gamma_{m,n}^{DUE} = \frac{P_{m,n} h_{m,n} g_{m,n}^{DUE}}{P_{l,n} h_{l,m,n} g_{l,m,n}^{DUE} + \sigma_n^2}$  we have  $\partial Q / \partial P_{l,n} > 0$  which states that  $Q(P_{m,n}, P_{l,n})$  is also

monotonically increasing on  $l_5$  with respect to  $P_{l,n}$ .

Overall,  $Q(P_{m,n}, P_{l,n})$  is either monotone or concave on the feasible region  $\partial \Psi$  and thus is quasiconcave on  $P_{l,n}$ . Due to symmetry, the above analyses also hold for  $P_{m,n}$ . According to [20],  $R_{m,l,n}(Q)$  is quasiconcave on  $\partial \Psi$  thus Lemma 3 holds.

#### D. Proof of Theorem 2

Proof: By using the statistical CSI  $\overline{h_{m,n} g_{m,n}^{DUE}}$  and  $\overline{h_{l,m,n} g_{l,m,n}^{DUE}}$ ,  $P_{m,n}^1$  and  $P_{l,n}^1$  are impacted and we denote them as  $\overline{P_{m,n}^1}$  and  $\overline{P_{l,n}^1}$ .

1)  $\overline{P_{m,n}^1} < P_{m,n}^1$ : This result decreases interference to the eNB and further increases transmission power of a CUE. Thanks to the maximum power constraint of  $P_{l,n} < P_{\max}^{CUE}$ , the expected performance of the LTE system will be reached at the cost of reduced D2D throughput.

2)  $\overline{P_{m,n}^1} > P_{m,n}^1$ : This case brings about higher D2D transmission power and thus more serious interference on the eNB. As a result, the LTE devices may go into outage where the eNB can not receive the data from the CUE successfully. In this case, the transmission power of the DUE must be restricted by the required QoS of the CUE.

3)  $\overline{P_{l,n}^1} < P_{l,n}^1$ : In this case, the cellular users will have outage because of lowered transmission power. So that the minimum transmission power of a CUE should be ensured.

4)  $\overline{P_{l,n}^1} > P_{l,n}^1$ : With a natural constraint of  $P_{l,n}^1 < P_{\max}^{CUE}$ , the LTE system will obtain better performance at the cost of decreased throughput of the D2D subsystem.

Based on the above analysis, we complete the proof.

## References

- [1] 3GPP TR 22.803 V0. 3.0, "3rd Generation Partnership Project; Technical Specification Group SA; Feasibility Study for Proximity Services (ProSe) (Release 12)," May, 2012.
- [2] S. Xu, H.M. Wang, and T. Chen, etc, "Device-to-Device Communication Underlying Cellular Networks: Connection Establishment and Interference Avoidance," *KSII TRANSACTIONS ON INTERNET AND INFORMATION SYSTEMS*, vol. 6, no. 1, pp. 203-228, Jan., 30, 2012.  
[Article \(CrossRef Link\)](#)
- [3] M. J. Yang, S. Y. Lim, and H. J. Park, etc, "Solving the data overload: Device-to-device bearer

- control architecture for cellular data offloading,” *IEEE Vehicular Technology Magazine*, vol. 8, pp. 31-39, Mar., 2013. [Article \(CrossRef Link\)](#)
- [4] G. Fodor, E. Dahlman, and G. Mildh, etc, “Design Aspects of Network Assisted Device-to-Device Communications,” *IEEE Communications Magazine*, vol. 50, no. 3, pp. 170-177, Mar., 2012. [Article \(CrossRef Link\)](#)
- [5] S. Wen, X. Zhu, and Z. Lin, etc, “Distributed Resource Management for Device-to-Device (D2D) Communication Underlay Cellular Networks,” in *Proc. of PIMRC 2013*, pp. 1624-1628, Sept., 2013. [Article \(CrossRef Link\)](#)
- [6] L. B. Le, “Fair Resource Allocation for Device-to-Device Communications in Wireless Cellular Networks,” in *Proc. of GLOBECOM 2012*, pp.5451-5456, Dec., 2012. [Article \(CrossRef Link\)](#)
- [7] J. Wang, D. Zhu, and C. Zhao, etc, “Resource Sharing of Underlying Device-to-Device and Uplink Cellular Communications,” *IEEE Communications Letters*, vol. 17, no. 6, June, 2013, pp. 1148-1151. [Article \(CrossRef Link\)](#)
- [8] C. Xu, L. Song, and Z. Han, etc, “Efficiency Resource Allocation for Device-to-Device Underlay Communication Systems: A Reverse Iterative Combinatorial Auction Based Approach,” *IEEE Journal on Selected Areas in Communications/Supplement*, vol. 31, no. 9, Sept., 2013, pp. 348-358. [Article \(CrossRef Link\)](#)
- [9] W. Fu, R. Yao, and F. Gao, etc, “Robust Null-Space Based Interference Avoiding Scheme for D2D Communication Underlying Cellular Networks,” in *Proc. of IEEE WCNC 2013*, pp. 4158-4162, Apr., 2013. [Article \(CrossRef Link\)](#)
- [10] H. Tang, C. Zhu, and Z. Ding, “Cooperative MIMO Precoding for D2D Underlay in Cellular Networks,” in *Proc. of IEEE ICC 2013*, pp.5517-5521, June, 2013. [Article \(CrossRef Link\)](#)
- [11] P. Phunchongharn, E. Hossain, and D. I. Kim, “Resource Allocation for Device-To-Device communications Underlying LTE-Advanced Networks,” *IEEE Wireless Communications*, vol. 20, no. 4, Aug., 2013, pp. 91-100. [Article \(CrossRef Link\)](#)
- [12] L. Su, Y. Ji, and P. Wang, etc, “Resource Allocation Using Particle Swarm Optimization for D2D Communication Underlay of Cellular Networks,” in *Proc. of IEEE WCNC 2013*, pp. 129-133, Apr., 2013. [Article \(CrossRef Link\)](#)
- [13] B. Kaufman, J. Lilleberg, and B. Aazhang, “Spectrum Sharing Scheme Between Cellular Users and Ad-hoc Device-to-Device Users,” *IEEE Trans. Wireless Commun.*, vol. 12, no. 3, pp. 1038-1049, March, 2013. [Article \(CrossRef Link\)](#)
- [14] S. Wen, X. Zhu, and Z. Lin, etc, “QoS-Aware Mode Selection and Resource Allocation Scheme for Device-to-Device (D2D) Communication in cellular networks,” in *Proc. of IEEE ICC 2013*, pp.101-105, June, 2013. [Article \(CrossRef Link\)](#)
- [15] Y. Chai, Q. Du, and P. Ren, “Partial Time-Frequency Resource Allocation for Device-to-Device Communications Underlying Cellular Networks,” in *Proc. of IEEE ICC 2013*, pp. 6055-6059, June, 2013. [Article \(CrossRef Link\)](#)
- [16] M. Belleschi, G. Fodor, and A. Abrardo, “Performance analysis of a distributed resource allocation scheme for D2D communications,” in *Proc. of IEEE GLOBECOM Workshops 2011*, pp.358-362, Dec., 2011. [Article \(CrossRef Link\)](#)
- [17] M. Zulhasnine, C. C. Huang, and A. Srinivasan, “Efficient resource allocation for device-to-device communication underlying LTE network,” in *Proc. of IEEE 6th International Conference on Wireless and Mobile Computing, Networking and Communications*, pp. 368-375, Oct., 2010. [Article \(CrossRef Link\)](#)
- [18] S. Sesia, I. Toufik, and M. Baker, *The UMTS Long Term Evolution: From Theory to Practice*, 2nd Edition, Wiley, 2011, ch. 5.
- [19] J. G. Andrews, F. Baccelli, and R. K. Ganti, “A tractable approach to coverage and rate in cellular networks,” *IEEE Trans. Commun.*, vol. 59, no. 11, pp. 3122-3134, Nov., 2011. [Article \(CrossRef Link\)](#)
- [20] S. Boyd and L. Vandenberghe, *Convex Optimization*, Cambridge University Press, 2004.
- [21] 3GPP TSG-RAN, “Technical Specification Group Radio Access Network; Further Advancements for E-UTRA, Physical Layer Aspects (Release 9)” *3GPP Technical Report, 3G TR 36.814, v9.0.0*, March 2010.

- [22] T. Chen, G. Charbit, and S. Hakola, "Time Hopping for Device-To-Device Communication in LTE Cellular System," in *Proc. of IEEE WCNC 2010*, pp. 1-6, Apr., 2010. [Article \(CrossRef Link\)](#)
- [23] 3GPP TS 36.213 v10.6.0, "Evolved Universal Terrestrial Radio Access (E-UTRA); Physical layer procedures (Release 10)," June 2012.



**Shaoyi Xu** received her Ph. D. degree from the Inha University, South Korea in 2007. After that, she worked in the Nokia Research Center in Nokia China Ltd. as a senior researcher and a postdoctor. From 2009 to now, she worked in the Beijing Jiaotong University. From Feb. 2013 to Feb. 2014, she is a visiting scholar in the Department of Electrical and Computer Engineering, University of California, San Diego, USA. She has obtained more than 20 international and Chinese patents and published more than 70 journal papers and conference papers. Her research interests include D2D communication, cooperative communication in high-speed environments, cognitive radio and UWB, etc.



**Kyung Sup Kwak** received the B.S. degree from the Inha University, Incheon, Korea in 1977, and the M.S. degree from the University of Southern California in 1981 and the Ph.D. degree from the University of California, San Diego in 1988. He is the current UWB Wireless Communications Research Center, a key government IT research center, Korea. He is now an Inha Fellow Professor (IFP). He was the KISC's president of 2006 year term. His research interests include multiple access communication systems, mobile communication systems, UWB radio systems, ad-hoc networks and high-performance wireless Internet.



**Ramesh Rao** earned his Ph.D. in Electrical Engineering from the University of Maryland, College Park in 1984, after receiving his M.S. from the same institution in 1982. He earned his Bachelor's degree in 1980 from the University of Madras. He has been a faculty member at UC San Diego since 1984, and Director of the Qualcomm Institute, UCSD division of the California Institute for Telecommunications and Information Technology (Calit2), since 2001. He also holds the Qualcomm Endowed Chair in Telecommunications and Information Technologies in the Jacobs School of Engineering at UCSD, and a member of the school's Electrical and Computer Engineering department. Dr. Rao is an IEEE Fellow and Senior Fellow of the California Council on Science and Technology. Among his most recent honors and distinctions, he received a 2011 Casa Familiar Abrazo Award for engagement with underprivileged area of San Diego. In his academic field of information theory, Dr. Rao has twice been elected to the IEEE Information Theory Society's Board of Governors and was Publications Editor for IEEE Transactions on Information Theory, as well as Guest Editor for a Special Issue on Multimedia Network Radio for the IEEE Journal of Selected Areas in Communications.